International Journal of
INTELLIGENT SYSTEMS AND APPLICATIONS IN ENGINEERING
ISSN:2147-6799 www.ijisae.org Original Research Paper

Microstructural characteristics of AA6061-T6 composite joints formed by friction stir welding process and with different nanoparticulate

Radhika Chada

Submitted: 11/11/2022 **Revised**: 20/12/2022 **Accepted**: 16/01/2023

Abstract. The mechanical properties of a Friction Stir Welded (FSWed) joint of AA6061-T6 alloy were attempted to be improved by refining the microstructure and confining the coarsening of strengthening precipitates at Nugget Zone (NZ) and heat-affected zone (HAZ). Nanomaterial reinforced friction stir welding was a new field that promises to improve joint quality by forming composite joints. AA6061-T6 alloy composite joints containing two different nano reinforcement particles (RP): Silicon Carbide (SiC) and Boron Carbide (B4C) at different weight ratio 5 wt%, 10 wt%, and 15 wt% were fabricated via friction stir welding process (FSW). Reinforcement particles (RP) particles were smaller than 1μm in size, the Zener pinning action prevented grain growth, which occurs during the FSW process's recrystallization stage, and limited grain coarsening by limiting grain boundary path motion. Microstructure analysis of all FSWed composite joints revealed a remarkable degree of grain refinement at the HAZ and NZ. Mechanical testing showed that while B4C particles had more advantage in terms of hardness values when compare with reinforcement of SiC particles. Similarly reinforcement of SiC particles had more advantage in terms of tensile strength of the FSWed composite joints when compared with reinforcement of B4C particles. The hardness of composite joints increased in direct proportion to the increase in volume fraction. The trend in tensile strength in composite joints was the inverse of the trend in hardness. FSW process created voids and crack initiation at the RP/BM matrix interface in 15% volume fraction composite joints due to the non-homogeneous distribution of nano particles and poor interaction. As a result, during the stress test, these joints fractured prematurely. The SEM was used to examine particle distribution in weld zone and fractured surfaces of all the tension test samples. Composite joints with a volume fraction of 5% to 10% exhibited uniform particle distribution and mixed ductile and brittle fractures

***Keywords**: Friction Stir Welded (FSWed), Reinforcement Powders (RP), Composite Joints, Grain Structure.*

1. Introduction

The joining of heat-treated alloys (AA6061-T6) by the Welding process often results in a deterioration of mechanical properties, since the strengthening precipitates are coarsening and dissolving (Mg_2Si, Al_3FeSi, $Al_{12}FeSi$) at the weld nugget. This problem confines the use of AA6061-T6 alloy. The AA 6061-T6 alloy is commonly used in the manufacturing industry due to a combine advantageous property such as high strength to weight ratio, good ductility, and low cost. The alloy is used to make aircraft wings and fuselages, as well as yacht construction and automobile wheel spacers. Due to potential damages during service and post-fabrication defects, repairs of AA 6061-T6 fabricated parts are sometimes needed [1, 2]. Due to the high propensity for solidification cracks and vaporization of alloying elements caused by high heat energy input, obtaining superior-quality welded joints of aluminum alloys through fusion welding is always a challenge. Solid state welding refers to a group of welding processes that produce coalescence at temperatures basically lower than the melting point of the base materials being joined, without the use of fluxes or other additives (filler metal) for welding. Friction stir welding is of solid state welding methods that are mainly used to weld the metal alloys, such as aluminum [3]. Strengthening precipitates greatly favor the heat-treatable aluminum alloy AA6082-T6. "- Mg5Si6 precipitates, which are the main strengthening precipitate stable below 200oC, are clearly visible in the microstructure[4].FSW differs from other welding technologies basically for materials with low on melting temperature. Low welding temperature, less deformation, fewer welding defects and easy to obtain welds with high mechanical properties are some of the benefits of this technique. In the FSW operation, the work piece is first touched by the spinning FSW tool, and the surface is then mechanical force is exerted against the interface of the joint. Because of the heat produced due to friction between the FSW tool and the base material, the material becomes softer. As the rotating tool moves transversely, increased recirculation of plastically deformed material forged in the front of the tool to the back of the tool – which caused plastic deformation – leads to heavy joining. [5].

Friction stir processing (FSP), branch of friction stir welding has recently been developed as an alternative for micro structural feature modification of various metals and alloys. To make a composite using FSP, slurry of the reinforcement particles (volatile solvent and mixer of

Assistant Professor of Department of Mechanical Engineering, Kakatiya University, Warangal, Telangana, India.
radhikareddy.chada@gmail.com

particle) applied as thin layer on the top surface of the Base metal (AA5083). They discovered a significant improvement in strength and micro hardness (175 HV) that are almost twice as high as the base material's (85 HV).This work reveals a variety of approaches and options for achieving uniform reinforcement particle (*RP*) dispersion in metallic-matrix. Attempts were also made to the development of bulk metal matrix composites (MMCs) using various methods FSP particle pre-deposition methods [6-7]. The expansion of these modern procedures was made to eliminate unnecessary operations and to prevent the loss of (*RP*s) during the process. Several studies have been done in the past based on the effective fabrication of various MMCs via FSP using various deposition techniques, such as the drilled holes process[6].groove method[7]direct coating [8]. However, the impact and function of nanoparticles on the mo*rp*hology and distribution of *RP*s in terms of precipitates in different zones of AA6061-T6-FSW joints has yet to be explored. The deposition method is critical for the durability, homogeneity, and spread ability of embedded *RP*s that may affect material attributes due to property gradients [9-10]. Radhika, et al [11] made a study on friction stir welded joint of heat-treated alloys (AA6061-T6) fabricated without and with four different reinforcement material (*SiC*, B_4C,Zn and Al_2O_3). Since the strengthening precipitates are coarsening and dissolving (Mg_2Si, $A_{l3}FeSi$, $Al_{12}FeSi$) , during stirring process of FSW, results a deterioration in mechanical properties at the weld nugget. To over this problem four butt joints of AA6061-T6 (FSW-*SiC* , FSW-Zn, FSW-B_4C, FSW-Al_2O_3) reinforced with *SiC*, B_4C,Zn and Al_2O_3 particles prepared by FSW process. Enhanced mechanical properties are observed in particle reinforced joints in comparison to unreinforced joint. Micro structure of reinforced joints also reveals a fine and equi axed grains in reinforced joint than un reinforced FSW joint, which is the reason for joint properties improvement. Among four reinforcement welds, FSW-B_4C joint comprises better strength and hardness values.

Until now, only a few studies on the mechanical characteristics of AA6061-T6 friction stir welds with reinforcement particles have been attempted. The technique, however, it is commonly employed to non-heat-treatable aluminum alloys, such as AA 5059[12], AA 5083 [13] and AA6061 [14] .since the reinforcement particles give the weldmets an extra improved strength. Aside from mechanical properties, wear resistance, which is a significant indicator of weld efficiency, is also enhanced. The wear resistance of these aluminum alloys reinforced with particles has been determined to be affected by particle size, shape, type, and volume. To enhance wear resistance, *SiC*, TiO_2, Al_2O_3 and other hard particles have been used as *RP* in friction stir welded joints of non-heat treatable aluminium alloys [14-15].

Tool geometry also plays important role in distribution of reinforcement particles which in turn decides mechanical and wear properties improvement of composites fabricated by FSW. Vahid M Khojastehnezhad [16] investigated the influence of various tool pin profiles on mechanical properties of surface hybrid composites of Al6061base and Al_2O_3–TiB_2 powder fabricated by friction stir processing. The results revealed that the more homogeneous dispersion of Al_2O_3–TiB_2 particles in Al6061base is achieved with square and triangular pin profiles tools because of sha*rp* edges and corners of the pin. The sharp edges of the pin causes excellent material flow and improved stirring of the material, which results a greater drop in particle clustering and the enhanced mechanical properties. Furthermore, the composite samples formed with square and triangular pin have more refined grains than the other composite samples. Due to finer grains, more uniform distribution of harder ceramic Al_2O_3–TiB_2 particles and reduced particle clustering, higher hardness and better wear resistance is observed in the composites fabricated with square and triangular pin profile. Several researchers used various methods to add *RP*s to parent-alloys. Sun et al [17] fabricated Cu matrix- composites in weld nuggets using a novel method involving FSW to integrate micro *SiC* particles in a distance of 1mm between the interfaces of the Cu plates.

However, the impact and effect of nano-sized Al_2O_3 particles on FSW the evolution of morphological grains geometry, RP dispersion in nano composites fabricated by FSW. Composites characteristics (mechanical) have yet to be explored. The deposition method is critical for the durability, distribution, and homogeneity of embedded RPs, which may affect material attributes depending on the property. [18].To this end, comparatively less work has been done on fabrication of composite joints of AA6061-T6 alloy with harder reinforcement material by FSW process. Thus this study aims to fill up and make a thorough evaluation of the feasibility of two different reinforcement powders of Silicon and Carbide Boron Carbide in fabricating composite joints by FSW process. The focus of the study is to investigate the influence of two different nano ceramic reinforcement particles at three different volume fraction (5% , 10%and 15%) on microstructural and mechanical properties of aluminum alloy 6061-T6 composite the gap joint fabricated via friction stir welding.

2. Experimental Procedure:

2.1. Material and Methods :

AA6061-T6 sheets were used as the Base metal with 6mm thickness for Friction stir welding. Nano powders of Silicon Carbide (SiC) and Boron

Carbide (B_4C) were used as reinforced materials for metal matrix composites. The % of chemical composition, physical and mechanical properties of AA6061-T6 alloy are shown in the Table 1. The SEM images of the reinforcement particles were shown in the Fig.1. The rolled AA 6061-T6 aluminum sheets were cut into the dimensions of length equal to 180mm and width equal to 60 mm. To integrate nano particles at the weld zone of the base plate, narrow slots with varying width and constant length and depth were made at the faying surface of the base material Fig. 2(a). The volume of the stir zone was equal to 5400 mm3 (length of the weld * depth of the nugget zone * width of the nugget zone).All the Base plates were cleaned and degreased with cleaning acetone solution and nano particle slurry was prepared by adding to acetone. The prepared nanoparticle slurry was compacted into the slots of the AA6061-T6 aluminum base plate. The nano particle-filled base plates were then dried in an oven at 60°C for 4 hours. The theoretical masses of reinforcement particles used for the fabrication of various nano composites were shown in the Table 2. However, due to particle loss during FSW, the actual mass concentration of nano particles may be slightly lower than the theoretical value. A vertical milling machine with attachments was used to fabricate metal matrix composite weld joint by FSW process. A square pin tool of 6mm side and 5.7mm depth had used for the FSW process Figure 2(b). Table 2 lists the embedded conditions as well as the specimen nomenclature. FSW was performed with a constant speed of 900 rpm, a 50mm/m feed rate, and a zero tilt angle. A single FSW pass was used for all of these combinations. All mechanical characterization was carried out in accordance with ASTM/ ASTME8M- 11 guidelines. Extracted samples of composite joints were etched for 10 to 15 seconds with 50ml HCl, 50ml Hno3, 50ml methanol, and 2-3 drops of HF to expose microstructure and related characteristics. Following that, optical microscopy and scanning electron microscopy (SEM: JCM-6000 plus 10X to 1lak) were used to classify the micro structural, particle distribution evolutions and the fractured surface of tensile samples. The welded samples tensile and mechanical properties were also assessed. The upper surface of welds was machined to remove rough impressions created by the shoulder surface before samples were prepared for the tensile examination. The macroscopic image of broken surfaces was studied after the tensile examination.

Table 1: The % of chemical composition and mechanical properties of AA6061-T6 alloy

Element	Al	Si	Fe	Mg	Mn	Zn	Cr
Wt%	Base	0.5	0.5	0.8	0.1	0.03	0.05

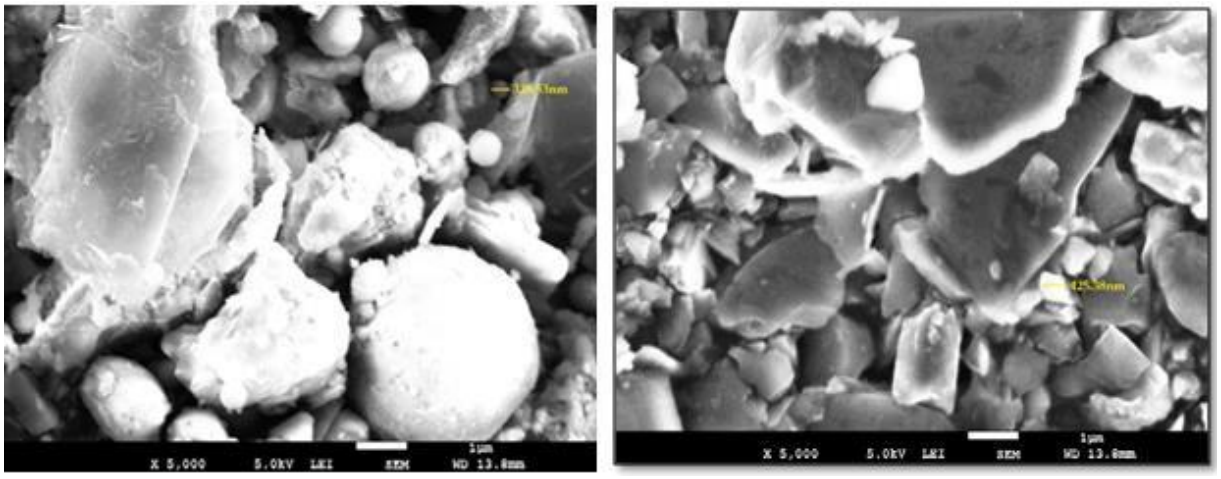

Fig 1: SEM images of reinforced particles a) *SiC* b) *B_4C*

Table 2: Processed material conditions for FSW

S.NO	Samples Conditions	Reinforcement Materials	Mass of SiC Nano particles added	Mass of B4C Nano particles added
1	AA 6061-T6-5wt%	SiC & B4C	0.824	0.578
2	AA 6061-T6-10wt%	SiC & B4C	1.646	1.154
3	AA 6061-T6 -15wt%	SiC & B4C	2.471	1.732

Fig 2. Processed materials across (a) Grooves prepared at joint interface for reinforcement materials (b) Square tapered tool used.

3. Results and Discussions:

3.1. Microstructure analysis:

This analysis aimed to determine the impact of each reinforcement particle's addition and to find the effect of *RP*. Before microstructure analysis, the developed composite joint samples were initially inspected visually. The surface appearance of the composite joints formed by FSW process with 15% volume fraction *RP* had an excessive lateral flash and a rough surface. A defect-free composite joint with a smooth surface appearance, no material splash, no voids, and tunnels has been identified within 5% and 10% volume fraction *RP* composite weld joints. The AA6061-T6 consists of strengthening precipitates and elongated grains of size *48*μmoriented in the rolling direction. Fig.4 (a).Due to extreme plastic deformation and recrystallization during the stirring stage of the FSW process results a reduces grain size structure. In addition to severe plastic deformation an impending effect of *RP* on grain boundary movement after recrystallization was leaded to even finer grains and equi- axed grains at *HAZ* and *NZ* of composite joints fabricated with FSW process Fig. 4 (a-f).

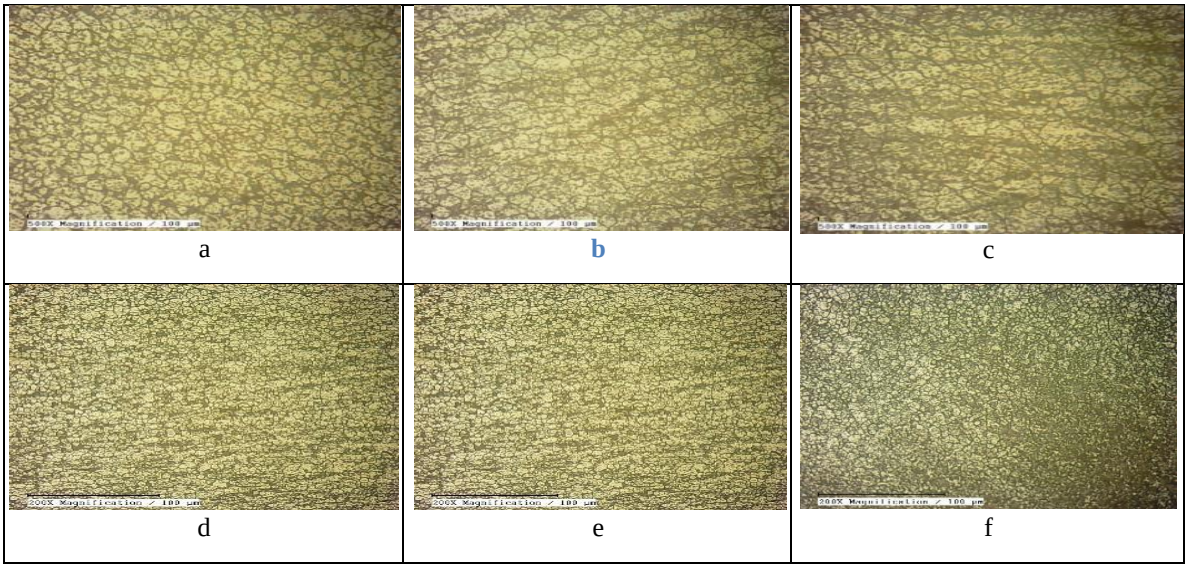

Fig.3. shows micro structure of base plate and NZ of joints: (a) rolled AA6061-T6 aluminium base plate, (b) unreinforced FSWed joint (c) CJ-5-SiC, (d) CJ-10-SiC, (d) CJ-15-SiC, (f) CJ-5-B_4C, (e) CJ-10-B_4C, (f) CJ-15-B_4C.

The purpose of this study is to depict the role and influence of nanoparticles in grain refinement of FSWed composite joints. Welded samples were cut perpendicular to the welding path with an electrical discharge machine to examine the distribution of RP through the welded joint. Figure 3(a-f) depicts macroscopic observations of joints along the cross-section of the weld at HAZ. The average grain size at various locations (HAZ, NZ) was calculated using image J software. This analysis considers the average grain size value. In NZ, the minimum reduction in grain size observed was(21 μm) in 5% volume fraction of SiC particles, while the maximum grain size reduction was observed (7 μm) at the highest volume fraction (15%) of B_4C particles. The number of reinforcement particles in the weld zone increases proportionally to the volume fraction percent of RP. As a Result, many nucleation sites formed in the weld zone, limiting grain growth and reducing grain diameter [17]. The grain size of the composite joints varied according to their microstructures, ranging from nanoparticle-rich to nanoparticle-free. In composite joints, the nanoparticle-

rich area (8-18 μm) had a smaller grain size compared to the nanoparticle-free region (23-28 μm). The Grain sizes of all manufactured FSWed composite joints were measured in HAZ and NZ (Fig. 3). Referring to Fig.3, it was discovered that in the FSW process, extensive plastic deformation promotes dynamic recrystallization (DRX) and continuous dynamic recrystallization (CDRX), resulting in the development of more refined grains with equiaxed at the weld zone of all composite joints. In addition to DRX and CRX, reinforced nanoparticles have a significant pinning effect on grain boundary migration, which leads to grain refinement in the NZ.

The study found that the FSW process, when combined with nano particle reinforcement, effectively refines the grain structure, improving the mechanical properties of AA6061-T6 composite joints. Because of the rotating tool's adequate stirring action, the base plate material deforms, allowing for better flow of reinforcement particles and grain refinement at the HAZ and NZ of FSW composite joints. Even although the same process parameters were used for all FSW composite joints, the presence of varying size fine grains in the nugget zone of various composite joints was attributed solely to the density of nano reinforcement particles. However, the particle stimulated nucleation (PSN) phenomenon is suitable for MMCs manufactured using the FSW process [23,24]. As dislocations accumulate at the reinforced particles during plastic deformation, the feasibility of PSN-based dynamic recrystallization becomes clear. According to Humphreys et al. [25], the most favorable conditions for PSN were larger reinforcement particles, low temperature, and severe deformation/high strain conditions. As a result, applying the PSN phenomenon to granular particles smaller than one μm proved challenging. As a result of the use of nano particles and a high processing temperature in the fabrication of FSW composite joints, the PSN effect was less likely in the current study. And due to the sufficient stirring action of the rotating tool, which deforms the Base plate material, the reinforcement particles flow more freely and the grain refinement at the HAZ and NZ of FSWed composite joints is improved [19].

About the microstructure of all FSWed composite joints, it was observed that the distribution of reinforced particles was more uniformly at *HAZ* and *NZ* of composite joints with 5% volume fraction *RP* and no variation in the dispersion/ agglomerations of nanoparticles. But because of asymmetry in the temperature distribution, the spread of *RP* particles was dispersed more towards the AS in comparison to the RS. The microstructure of *CJ*-5-*SiC* (Fig.3.c.) joints revealed that nodular grains with uniform distributed *SiC* particles at the grain boundaries. The same phenomenon was observed in *CJ-10-SiC* joints except for slightly increased size grains. But in the case of the *CJ-15-SiC* joint, the same nodular grains with very few particle agglomerations were observed. while the microstructure of *CJ*-5- B_4C composite joint (Fig.4.f) consist of a mixture of nodular and sharp fine grains with the distribution of B_4C particles were uniform at *NZ* and no variation in the dispersion/ agglomerations of nanoparticles. The microstructure at *NZ* was similar to that of *HAZ*, but with larger grain sizes, as shown in Fig.3.(a-f). In terms of particle distribution, *HAZ* had a less number *RP* spread than the distribution at *NZ* of all FSWed composite joints. As a result, differences in grain size were observed between HAZ and *NZ* of all FSWed composite joints. Fig.4.d. indicates the distribution of B_4C particles were uniform at *NZ* of *CJ*-10-B_4C composite joint, and finer grain structure than *CJ*-5-B_4C composite joints. In 15% volume fraction B_4C particle composites much finer grains of 8-16 μm size was observed at *NZ* of joint. These results confirm that both types of *RP* (*SiC*, *B4C* particles with 5% and 10% volume fractions) influenced the refinement of microstructures of FSWed composite joints But as discussed earlier i.e., because of asymmetry in the temperature distribution, the spread of B_4C particles were dispersed more towards the advancing side (AS) in comparison to the retreating side (RS). Along with the temperature difference created by the spinning tool's motion, the material on the AS was squeezed to the tool's back in a counter-clockwise movement direction. Fig.3 (a-f). Depicts the difference in average grain size at *HAZ* and *NZ* as a function of type and volume fraction of reinforcement particles. It shows that, as the percentage of *RP* in the composite material increases, the *NZ* grain size decreases. The finer grain size order of composite joints concerning to type of *RP* was in the order of B_4C particle reinforced joints followed by SiC reinforced composite joints.

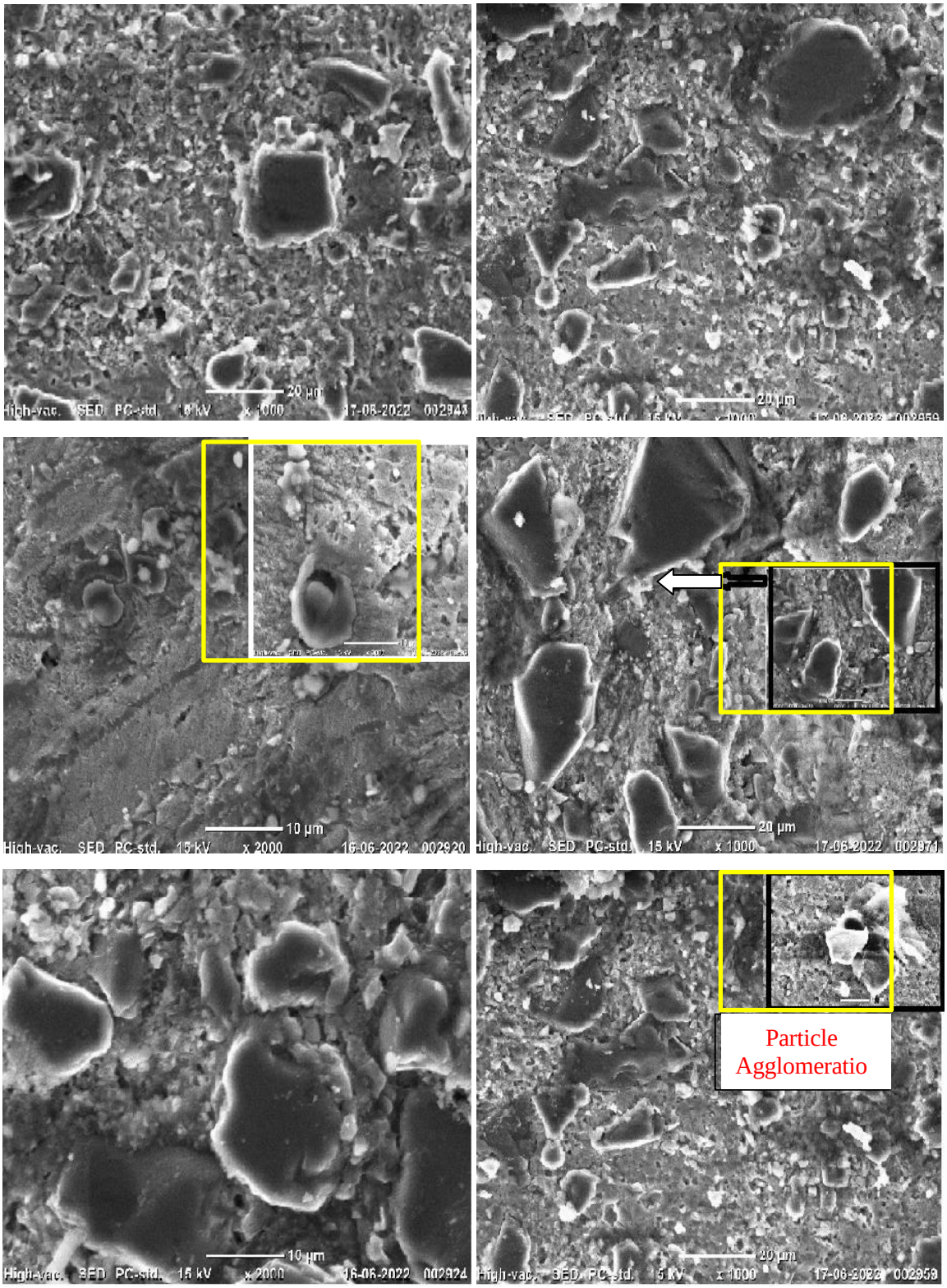

Fig.4. SEM structures shows particle distribution at NZ of Composite joints (a)*CJ*-5- *SiC*,(b)*CJ*-10-*SiC*,(c)*CJ*-15-*SiC*, (d) *CeJ*-5-B_4C,(e)*CJ*-10-B_4C, (f) *CJ*-15- B_4C.

However, the distribution of reinforced nanoparticles was a major concern when making composite joints. The uniform distribution of nanoparticles in the weld zone was influenced by parameters such as the volume fraction of RP, pin profiles, and the number of weld passes. Even though the same process parameters were employed for all FSWed composite joints, The occurrence of varied size fine grains in the nugget zone of different composite joints was attributed only due to the existence of varied density of nano reinforcement particles. According to the literature, the most suitable pin profiles for uniform distribution are square or hexagonal shapes. Hence All composite joints were fabricated using a tapered square pin profile and a single pass. The sharp edges of the tool pin contribute to a uniform distribution of RP at the weld zone [16].

Although, particle stimulated nucleation (PSN) phenomenon worthy for MMCs fabricated by the FSW process [23,24].As dislocations begin to accumulate at the reinforced particles during plastic deformation, however, the feasibility of PSN-based dynamic recrystallization becomes apparent. Following Humphreys et al[25], the most suitable conditions for PSN were larger reinforcement particles, low temperature, and severe deformation//high strain conditions. Hence It was difficult to occur PSN phenomenon for the particle granularly size having less than $1\mu m$. Therefore due to the use of nanoparticles and high processing temperature for the fabrication of FSWed composite joints, the PSN effect was more improbable in the present study**.** Thus the cause for finer grain size in the *NZ* of composite joints made with *SiC*, B_4C particles were more connected to the presence of nanoparticles. The nanoparticles act as an impediment to the movement of grain boundaries via a phenomenon known as Zener-pinning, resulting in finer grains at the stir zone [17,25]. which exerts a pinning force or pressure on the movement of both high and low angle grain boundaries by influencing the distribution of finer particles by opposing the driving force which moves the grain boundaries.

About the microstructure of all FSWed composite joints, it was observed that the distribution of reinforced particles was more uniformly at *HAZ* and *NZ* of composite joints with 5% volume fraction *RP* and no variation in the dispersion/ agglomerations of nanoparticles. But because of asymmetry in the temperature distribution, the spread of *RP* particles was dispersed more towards the AS in comparison to the RS. The microstructure of *CJ*-5-*SiC* (Fig.4.c.) joints revealed that nodular grains with uniform distributed *SiC* particles at the grain boundaries. The same phenomenon was observed in *CJ-10-SiC* joints except for slightly increased size grains. But in the case of the *CJ-15-SiC* joint, the same nodular grains with very few particle agglomerations were observed. while the microstructure of *CJ*-5- B_4C composite joint (Fig.4.f) consist of a mixture of nodular and sharp fine grains with the distribution of B_4C particles were uniform at *NZ* and no variation in the dispersion/ agglomerations of nanoparticles. The microstructure at *NZ* was similar to that of *HAZ*, but with larger grain sizes, as shown in Fig.4.(a-f). In terms of particle distribution, *HAZ* had a less number *RP* spread than the distribution at *NZ* of all FSWed composite joints. As a result, differences in grain size were observed between *HAZ* and *NZ* of all FSWed composite joints. Fig.4.e. indicates the distribution of B_4C particles were uniform at *NZ* of *CJ*-10-B_4C composite joint, and finer grain structure than *CJ*-5-B_4C composite joints. In 15% volume fraction B_4C particle composites much finer grains of 8-16 μm size was observed at *NZ* of joint. These results confirm that both types of *RP* (*SiC*, *B4C* particles with 5% and 10% volume fractions) influenced the refinement of microstructures of FSWed composite joints But as discussed earlier i.e., because of asymmetry in the temperature distribution, the spread of B_4C particles were dispersed more towards the advancing side (AS) in comparison to the retreating side (RS). Along with the temperature difference created by the spinning tool's motion, the material on the AS was squeezed to the tool's back in a counter-clockwise movement direction. On the other hand, the plastized material was extruded on the tool's rear in a clockwise direction on the RS during stirring operations. As a result of the forward tool movement, the deformed material is dispersed more towards the AS[9,29]. As a result, the microstructure of all composite joints revealed that reinforcement particles were distributed slightly more on the advancing side than on the retreating side. Composite joints with fractions (5% and 10%) provide uniform particle distribution and improved mechanical properties, whereas higher volume fractions (15%) cause agglomeration and potential defects. Comparison of SiC and B_4C reinforcements reveals that both particles effectively reduce grain size, with SiC having slightly better distribution and less agglomeration tendency at higher concentrations. This detailed SEM analysis emphasizes the importance of adjusting reinforcement particle concentration in FSWed composite joints to achieve the desired mechanical properties and structural integrity. The agglomeration of particles in joints made with 15% volume fraction RP, as shown in Fig.4(c&f). Particle agglomeration results in microvoids or cracks due to poor cohesion between the reinforced nano-particles and the metal matrix. In contrast, reinforced composite joints with a 5% volume fraction showed uniform particle distribution.

Concerning to the asymmetry in the temperature distribution, RP particles spread more towards the AS than the RS. Microstructure of CJ-5-SiC joints (Fig.4.c.) showed nodular grains with uniformly distributed SiC particles at the grain boundaries. Same phenomenon was observed in CJ-10-SiC joints, with the exception of slightly larger grains. same nodular grains with few particle agglomerations. microstructure of the CJ-5-B_4C composite joint (Fig.4.f) is a mixture of nodular and sharp fine grains, the distribution of B4C particles is uniform at NZ, and there no variation in the dispersion/agglomeration of nanoparticles. microstructure at NZ was similar to that at HAZ, but with larger grain sizes, as shown in Figure 5. of particle distribution, HAZ had a lower RP spread than the NZ distribution of all FSWed composite joints. result, grain size differences were found between HAZ and NZ of all FSWed composite joints. that the distribution of B4C particles was uniform at the NZ of the CJ-10-B4C

composite joint, with a finer grain structure than the CJ-5-B4C composite joints. fraction B4C particle composites, finer grains of 8-16 μm size were observed at the NZ of the joint. results confirm that both types of RP (SiC and B4C particles with 5% and 10% volume fractions) influenced the refinement of microstructures in FSWed composite joints. previously discussed, due to asymmetry in the temperature distribution, B4C particles were distributed more towards the advancing side (AS) than the retreating side (RS). with the temperature difference caused by the spinning tool's motion, the material on the AS was squeezed to the tool's back in an anticlockwise direction.

3.2. Tensile Properties:

Tensile properties of the FSWed composite joints were influenced by various factors like presence of hardened precipitates, grain size, dispersion of reinforced particles in the base plate material and weld defects in the joints. The grain refinement and solution treatment effect of *RP* had made all the FSWed composite joints to brittle. Hence B_4C composite joint with highest RP was showed a reduced tensile properties than un reinforced FSW joint. As mentioned earlier pinning effect of *RP* such as *SiC*, B_4C could confine sliding of the grain boundary path and dislocation movement and resulted a finer grain structure.

In addition, combined with a weak interfacial bond between the nano particles and the BM, the tensile properties of FSWed composite joints deteriorate. Furthermore the grain shape also influence tensile properties of the composite joints. The refined grains in composite joints were due to *RP* that accumulated at grain boundaries and acted as an obstacle to dislocation movement and grain growth, causing the current material to harden [24,26]. Since precipitation particles vary in structure and size, finely scattered second phase nanoparticles cause lattice distortion. Such defects caused by dislocations produced a stress field (tensile and compressive stress) around the dislocations[20,22]. As a result of these conditions, both positive and negative interaction energy between precipitates and dislocations was accumulated. As a consequence, depending on the size of the nanoparticles, the dislocations either attract or repel the precipitates, resulting in one of two situations: increased or decreased strength.Fig.(7). displays the measured tensile properties of FSWed composites joints. The results revealed that FSWed joints with and without nanoparticles reinforcement have different strength values.*SiC*composite joint produced with 5% RP showed higher strength of *217.6Mpa* , most likely due to the nodular shape finer grains and are more uniform spread of *SiC* particles under these processing parameters.The lowest strength was achieved with *CJ-15-*B_4C joint, because of the brittle nature of B_4C particles, led to more unlikely condition for PSN recrystallization phenomenon[25].

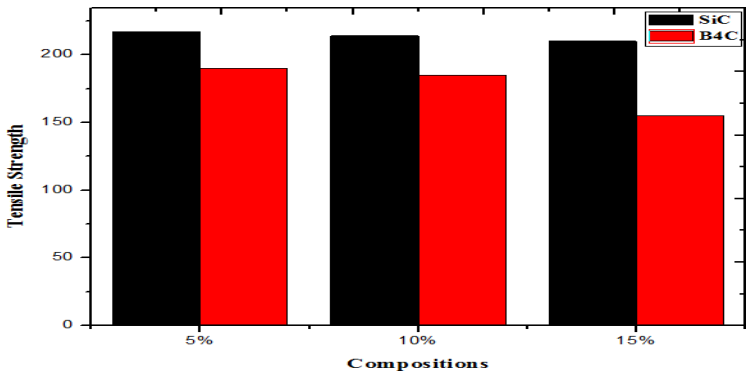

Fig 7. Shows the UTS of SiC and B_4C particle reinforced composite joints with three varying volume fractions.

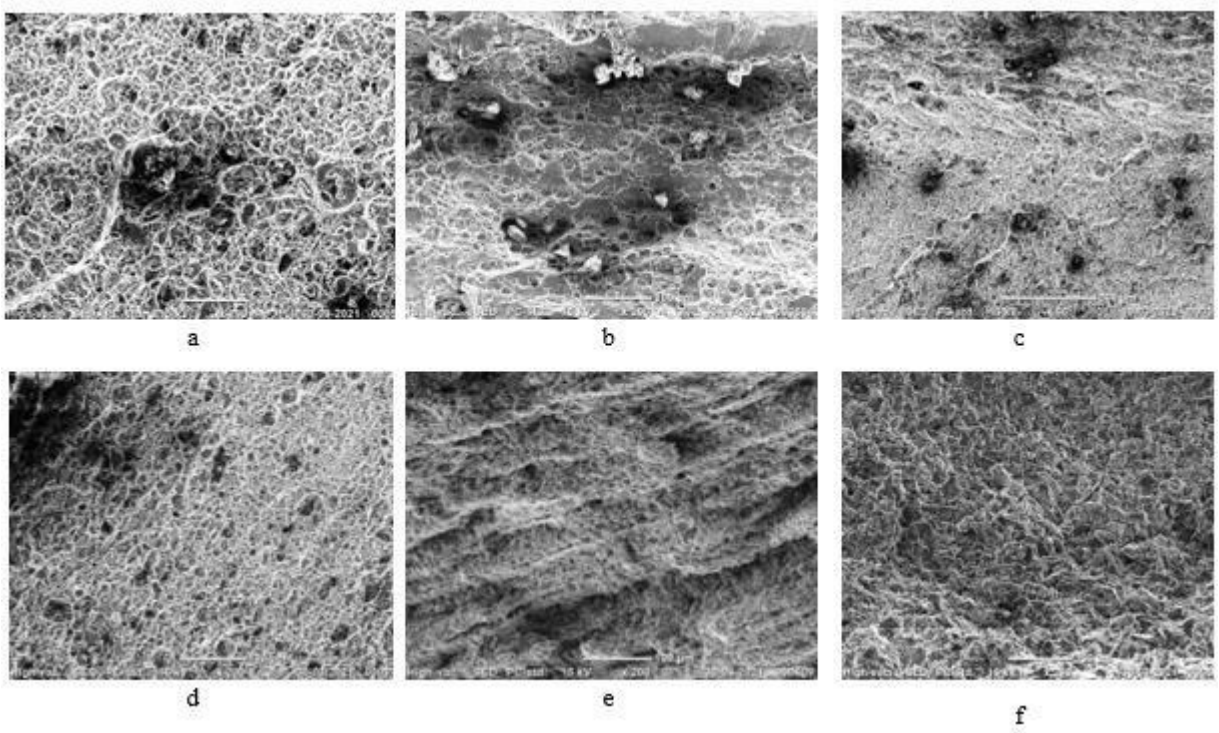

Fig 8.SEM images of fractured surface of composites joints reinforced a) *CJ*-5-*SiC*, (b)*CJ*-10-*SiC*, (c)*CJ*-15-*SiC*, (d) *CJ*-5-B_4C, (e)*CJ*-10-B_4C, (f) *CJ*-15-B_4C.

So as to better comprehend the effect of microstructure on the failure pattern of FSWed composite joints, a failure analysis was conducted. SEM was used to analyze the fracture surfaces of broken tensile specimens. Changing the reinforcement volume fraction percent had a key impact on the fracture pattern of FSWed composite joints, as shown in Fig.8.When considering the second phase reinforcement particles as void nucleation sites, the number of void nucleation sites increases as the particles disperse. As a result, the dimples will start out small and join up with the adjacent voids before becoming larger [27].A ductile mode fracture is indicated by the large shaped void and thick ridge of tear in the *SiC* particles reinforcement composite joints(Fig8.a-c).Fig.8.d-f. indicates the voids in the surface of the B_4C nanoparticles composite joints were smaller, resulting in combine nature fracture(brittle and ductile). Moreover in the B_4C reinforcement particle composite joints, smaller grain size leads to the shallower dimples and few particle agglomeration the probability of failure was combine ductile and brittle manner as shown by the existence of dimples. However the major portion of fracture in B_4C composites was due to brittle except at the *HAZ*(less brittle area). The FSW process formed porosities and cracks in the B_4C composite joints due to highly non-homogeneous distribution caused by poor interfacial bonding between the scattered B_4Cparticles and the BM and particle agglomerations shown in Fig.8.f. As a result, absolute brittle premature fracture in CJ-15-B_4C composite joint was observed.

3.3. Micro Hardness:

The measured values of Vickers's micro hardness of base material, FSW joints without reinforcements, and FSW composite joints with two different reinforcements were shown in Fig.9.a&b. According to the hardness findings, it was clear, the addition of all two types of nanoparticles significantly improved the micro-hardness of the FSW composite joint at all zones *HAZ (RS), HAZ (AS)*, and *NZ*. The intrinsic properties of nanoparticles, such as very high hardness values, uniform dispersion of SiC and B_4C particles, and PSN/Zener-pin-effect (ZPE) caused by RP, increased the micro hardness of the FSWed composite joint. According to the PSN phenomenon, the accumulation of nanoparticles behaves as the most preferential site for nucleation and growth. This results in the formation of new equiaxed refined grains after DRX [20, 22]. After DRX and grain growth stage, every single added nanoparticle helps in restrain the grains coarsening by providing the obstruction to the grains boundaries path which results in fine grain size, via ZPE, although such reinforced nanoparticles already have a higher inbuilt hardness distribution [21] which acts as an additional impediment to the dislocation density's motion.

Fig.9 (a &b) Indicates the micro-hardness values measured at HAZ and *NZ* of all FSW composite joints with 5% *RP*. In contrast to the nano particle-free FSW joint, FSW composite joints prepared with nanoparticles had finer size grained structured. As a consequence of the fine equiaxed grains, the hardness was increased. The

micro-hardness of the advancing side *(AS)* was higher than the retreating side *(RS)* when nanoparticles were incorporated. This was due to unevenness temperature distribution and difference in velocity of the particle (more at RS/less at AS) between *AS* and *RS* results in more extraction of plasticized base material and reinforcement particles on the advanced side than RS. [11, 17, 22]. As a consequence of the irregular circulation of the plastically deformed material, more nanoparticles would be distributed on Advancing Side. As a result, the hardness values in *AS* were higher than those in *RS*. The composite joint's hardness was proportional to the volume fraction percentage. The hardness of the composite join increased as the volume fraction increased. Along with the volume fraction of RP, the type of reinforcement had an effect on the hardness of the FSWed composite joints. Finely formed composites had the highest hardness values. The smaller the grain size, the higher the hardness value. B_4C composite joints had the smallest grain size *(8µm)* according to grain measurement estimates. As a result, B_4C composite joints have higher hardness values. The *SiC* particle reinforced composite joints displayed lesser hardness values and high strength. Another aspect that affected the hardness value was the distribution of nanoparticles. Particle-rich and particle-free zones resulted from composite joints with non-uniform nanoparticle distribution. As a result, hardness values were higher in particle-rich regions and lower in particle-free regions. Such variations were observed on both sides of the stir zone. In contrast, unreinforced FSW joints in the Nugget zone showed a stable hardness distribution.

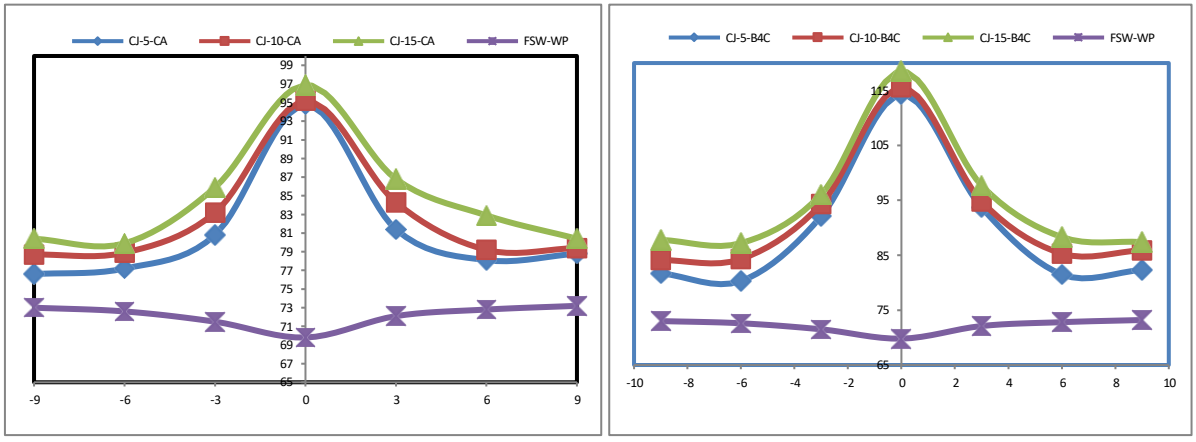

Fig.9.a Indicates Hardnesss variation on advanced and retreating side of (a). SiC particle reinforced composite joints (b) B4C particle reinforced composite joints

4. Conclusions

In this analysis, the effects of two different types of nanoparticles (*SiC*and B_4C particles) added at three different volume fractions (5%, 10%, and 15%) on the microstructure, mechanical, and microstructural properties of AA6061 aluminum alloy composite joints fabricated by fraction stir welding method were investigated. The finding of mechanical testing's revealed that an increment in hardness and strength properties of AA6061-T6 alloy composite joints as compare to FSW joints prepared without nano-particles. The following conclusions have been drawn from the existing research: After Friction stir welding, the nugget zone of AA6061-T6 composite joints fabricated with a 5% volume fraction of *RP* showed a uniform distribution of nanoparticles and no formation of particle agglomerates. Every added nanoparticle helps to prevent grain coarsening by obstructing the grain boundaries path, resulting in fine grain size. via Zener-pin-effect. As a result, all nanoparticle-reinforced AA6061-T6 composite joints had smaller grain sizes at *NZ* and *HAZ* than unreinforced FSW joints. The existence of harder nano *RP*, material grain refinement attributed to particle stimulated nucleation (PSN), and the occurrence of solid ceramic bonding through the Zener-pin-effect resulted in increased hardness values in welded composite joints. However, there was a difference in hardness value between the Advanced and Retreating sides of the weld zone, as well as between the particle-free and particle-rich zones. Unreinforced FSW joints had uniform micro hardness values at the weld nugget area, whereas FSWed composites joints did not. The effects of different reinforcement particles on hardness values were in the order of B_4C reinforced composite joints followed by SiC reinforcement particle composite joints. It appears that the hardness of *RP* affects the hardness of composite joints as well. A closer view clearly explained that B_4C particles had a bit more influence on hardness values of FSWed composite joints compare to those other nanoparticles. The results also revealed that the volume fraction of reinforcement material also had a major impact on the strength and

hardness values of FSWed composite joints, in addition to the variety of reinforcement materials. The hardness of the composite joint improved as the volume fraction of reinforcement material increased. However, more amounts of particle rich and particle-free zones were resulted in 15% volume fraction *RP* composite joints due to inadequate stirring action and low cohesion between base AA6061-T6 alloy material and reinforcement particles. As a result, the 15% volume fraction composite joints had a large variance in hardness values. Thus, the mean hardness values of these joints were nearly equal to composite joints with a 10% volume fraction. The higher hardness (118HV) was obtained by using a 15% volume fraction of B_4C particle composite joints (*CJ*-15-B_4C) and the *CJ*-5-*SiC* composite joint had a lower hardness (81.8HV*)*. When compared to the hardness of the FSWed joint without *RP* (*78HV*), the *CJ*-15-B_4C joint improved by *51%*, and even the lower hardness joint improved by *15%*.hardness than was observed. The addition of nanoparticles had less of an impact on the tensile properties of the FSWed composite joints. Adding harder nano *RP* to FSWed AA6061-T6 joints rendered them brittle. When compared to the B_4C nanoparticles, the addition of SiC nano-particles improved the tensile strength of FSWed composite joints, but the addition of B_4C did not affect the tensile strength properties. As a result, the tensile strength of the *SiC* particles reinforced composite joint *(CJ-5-SiC)* had been showed highest (213Mpa), while the B_4C particle reinforced composite joints *(CJ-15- B_4C)* had the lowest value (154.35Mpa). The volume fraction of *RP* also made an impact on tensile strength FSWed composite joints, but the trend was opposite to the hardness trend, i.e, the strength of composite joints decreased as the volume fraction increased. As a result, the strength values of 15% volume fraction *RP* composite joints were lower than the other two-volume fraction composite joints (*5% and 10%).*

References

[1] S Rajakumar, C Muralidharan, Balasubramanian V.Establishing ., 2010, "empirical relationships to predict grain size and tensile strength of friction stir welded AA 6061-T6aluminium alloy joints. " Trans Nonferrous Met Soc China., 20 (10) pp. 1863–72.

[2] M Marini, Ismail AB. Torsional., 2011, "deformation and fatiguebehaviour of 6061 aluminium alloy." IIUM Eng J. 12 pp. 21–32.

[3] Ch. Radhika , N. Shyam kumar. ,2019, " Process Parameters Optimization of Aa2024 Alloy Friction Stir Welding using Taguchi's Technique, " International Journal of Innovative Technology and Exploring Engineering 8 pp. 1940-45.

[4] P. M. G. P. Moreira, T. Santos, S. M. O. Tavares, V. Richter- Trummer, P. Vilaça and P. M. S. T. de Castro.,2009, "Mechanical and metallurgical characterization of friction stir welding joints of AA6061-T6 with AA6082-T6." Mater. Des. 30 pp. 180-187 .

[5] D. Lohwasser, Z. Chen., "Friction Stir Welding from Basics to Applications", CRC, 2010.

[6] J. Gandra, R.Miranda, P. Vilac, A.Velhinho, P.T.J., 2011,"Producing, Functionally graded materials by friction stir processing." J. Mater. Process. Technol . 21(11) pp. 659–1668.

[7] C.M.A. Fernández, R.A. Rey, M.J.C. Ortega, D. Verdera, C.L. Vidal., 2018, "Friction stir processing strategies to develop a surface composite layer on AA6061-T6.", Mater. Manuf. Process. 33 (10) pp.1–8.

[8] Sharma, V.M. Sharma, S. Mewar, S.K. Pal, J. Paul., 2018,"Friction stir processing of Al6061- *SiC* - graphite hybrid surface composites." Mater. Manuf. Process. 33 (7) pp. 795–804.

[9] P. Karthikeyan, K. Mahadevan., (2015, "Investigation on the effects of *SiC* particle addition in the weld zone during friction stir welding of Al 6351 alloy." Int. J. Adv. Manuf. Technol. 80 (9–12) pp. 1919–1926.

[10] J. Guo, B.Y. Lee, Z. Du, B. Guijun, J.M. Tan, W. Jun., 2015," Effect of nano-particle addition on grain structure evolution of friction stir processed Al 6061 during post-weld annealing." Arab. J. Sci. Eng. 40 (2) pp.559–569.

[11] Radhika. Chada, N. Shyam kumar., 2020," Investigation of micro structure and mechanical properties of Friction stir welded AA6061 Alloy with different particulate reinforcements addition." Edit pdf JOURNAL OF MECHANICS OF CONTINUA AND MATHEMATICAL SCIENCES. 15 pp. 264-278.

[12] M Srivastava , Sandeep Rathee., 2020,"A Study on the Effect of Incorporation of SiC Particles during Friction Stir Welding of Al 5059 Alloy ". Springer Nature B.V., pp.66.

[13] S . Sajad Mirjavadi, Mohammad Alipour, Soheil Emamian et al., 2017," Influence of TiO_2 nanoparticles incorporation to friction stir welded 5083 aluminum alloy on the microstructure, mechanical properties and wear resistance ". Journal of Alloys and Compounds . 712 pp.795–803.

[14] Radhika Chada, N. Shyam Kumar.,2022 ' Investigation of micro structural characteristics of friction stir welded AA6061 joint with different

particulate reinforcements addition'. AIP Conference Proceedings, 2418(1), pp. 050010-1-10.

[15] Seyed Sajad Mirjavadi, Mohammad Alipour, Soheil Emamian, S. Kord, A.M.S. Hamouda, Praveennath G. Koppad, R. Keshavamurthy.,2017'Influence of TiO2 nanoparticles incorporation to friction stir welded 5083 aluminum alloy on the microstructure, mechanical properties and wear resistance,Journal of Alloys and Compounds, 712 pp 795-803

[16] R.Srinivasan,M.Vesvanth,Kv.Sivasuriya,S.Sanjay, M.J.VineshMadhu.,2020,"Experimental investigation on the effect of tool rotation speed on stir cast friction stir welded aluminium hybrid metal matrix composite". Materials Today: Proceedings.22(14) pp.7843-7853

[17] M .Vahid Khojastehnezhad1, Hamed H Pourasl1 and Reza Vatankhah Barenji., 2017 "Effect

of tool pin profile on the microstructure and mechanical properties of friction stir processed Al6061/Al_2O_3—TiB_2surface hybrid composite layer". J Materials: Design and Applications. 0(0) pp.1–13.

[18] H.M. Rajan, I. Dinaharan, S. Ramabalan, E.T. Akinlabi., "Influence of friction stir processing on microstructure and properties of AA7075/*TiB2* in situ composites, J.Alloys Compd. 657 (2016) 250–260.

[19] Hsu *CJ*, Chang CY, Kao PW and Chang CP., 2006,"Al–Al_3Ti nano composites produced in situ by friction stir processing". Acta Mater. 54 pp. 5241–9

[20] Q. Hu, H. Zhao, F. Li., 2016,"Effects of manufacturing processes on microstructure and properties of Al/A356–*B4C* composites, Mater." Manuf. Process. 31 pp.1292.

[21] M. Bodaghi, K. Dehghani., 2016,"Friction stir welding of AA5052: the effects of *SiC* nanoparticles addition." Int. J. Adv. Manuf. Technol. 88 pp.2651–2660.

[22] Devaraju, A. Kumar., 2011,"Dry sliding wear and static immersion corrosion resistance of aluminum alloy 6061-T6/*SiC*p metal matrix composite prepared via friction stir processing." Int JAdv Res Mech Eng . 1 (2) pp. 62–68.

[23] Y. Morisada, H. Fujii, T. Nagaoka, M. Fukusumi., 2006,"Nanocrystallized magnesium alloy uniform dispersion of C60 molecules." Scr. Mater, pp.1067–1070

[24] J.M. Root, D.P. Field, T.W. Nelson., 2009,"Crystallographic texture in the friction-stir welded metal matrix composite Al6061 with 10 vol pct *Al2O3*," Metall. Mater. Trans, A .40 (9) pp.2109–2114.

[25] J. Guo, P. Gougeon, X.G. Chen., 2012 ,"Microstructure evolution and mechanical properties of dissimilar friction stir welded joints between AA1100-*B4C* MMC and AA6063 alloy." Mater. Sci. Eng A.553 pp. 149–156.

[26] F.J. Humphreys, M. Hatherly, 2004, Chapter 13 - hot deformation and dynamic restoration,in: Recrystallization and Related Annealing Phenomena, Elsevier Ltd. pp. 415–450.

[27] C.J. Tweed, B. Ralph, N. Hansen., 2004," The pinning by particles of low and high angle grain boundaries during grain growth." Acta Metall. 32 (9) pp. 1407–1414

[28] M . Barmouz, Givi, M.K.B, Seyfi. J., 2011, 'On the role of processing parameters in producing Cu/*SiC* metal matrix composites via friction stir processing::Investigating microstructure, microhardness, wear and tensile behaviour". Mater. Charact. 62 pp.108– 117.

[29] Radhika Chada, N. Shyam Kumar.,2022 ' Micro structural characteristics of dissimilar friction stir welds between AA7475- T7651 and AA6061-T6 aluminium alloys'. AIP Conference Proceedings, 2418(1), pp. 050091-9.